Chapter 3

α-Synuclein Membrane-bound Structures Characterized by Fluorescence Energy-transfer Kinetics

3.1 ABSTRACT

A hallmark of Parkinson's disease is the presence of fibrillar protein deposits in the brain, composed mostly of α-synuclein. Although its function is unknown, α-synuclein is found to associate with synaptic vesicles. Interestingly, α-synuclein appears to be natively unfolded *in vitro*. However, in the presence of membrane mimics, such as SDS micelles and acidic phospholipid vesicles, α-synuclein adopts a highly helical conformation. We have characterized the structures of α-synuclein variants, incorporated with tryptophan and 3-nitrotyrosine as donor and energy acceptor pairs, in the presence of SDS micelles and small unilammelar vesicles by time-resolved fluorescence energy-transfer measurements. Distance distributions extracted from these data provide site-specific information on the protein conformations.

3.2 INTRODUCTION

Previously, Ulmer et al. have employed NMR to characterize the structure of α-syn in the presence of SDS micelles.[1] The 20 lowest conformations of the structure (PDB file: 1XQ8) demonstrated that α-syn forms two helices, residues 3-37 (referred to as the N-terminal helix) and residues 45-92 (referred to as the C-terminal helix). These two helices are arranged in an antiparallel fashion and joined by a linker consisting of residues 38 through 44. The highly acidic C-terminal tail remains unstructured.

On the other hand, Langen et al. have investigated the structure of α-syn in the presence of acidic small unilammelar vesicles (SUVs) using EPR.[2] They concluded that residues 8 to 89 arrange themselves into three helices every 11 amino acids (α11/3 helices). They have also observed the formation of the motif of two helices and a linker. However, the helices do not arrange themselves in an antiparallel fashion.

SDS micelles have been typically estimated to have a circumference of 15 nm,[3] while the SUVs used for this study are approximately ten times larger in surface area. Since micelles are much smaller in size compared to SUVs, it was suggested by Bussell et al. that α-syn must adopt a more compact structure when it is associated with micelles.[4] They also reported that α-syn forms α11/3 helices in the presence of micelles and SUVs.

Time-resolved fluorescence energy-transfer (FET) has been employed to determine the structure and dynamics of α-syn in solution, SDS micelles, and acidic SUVs. Since FET rate is inversely proportional to the sixth power of fluorescent

donor-acceptor (D-A) distances,[5] it is possible to extract probability distributions of D-A distances from the fluorescence decay kinetics.[6-9] Fluorescent donor and energy acceptor chosen for this study were the fluorescent amino acid tryptophan (Trp) and a chemically modified tyrosine (Tyr), 3-nitrotyrosine [Y(NO_2)], respectively. This D-A pair has a Förster distance of 26 Å,[10] with a maximum extractable distance of 40 Å.

Six D-A pairs have been placed in strategic positions to probe the behavior of α-syn in sodium phosphate (NaP_i) buffer, SDS micelles, and acidic SUVs. The positions of the mutations have been highlighted in **Figure 3.1.**[11] W4/Y19(NO_2) and Y19(NO_2)/W39 were engineered to examine the N-terminal helix, while Y39(NO_2)/W94 and Y74(NO_2)/W94 were for C-terminal helix. W39/Y55(NO_2) was used to probe the linker region. W4/Y94(NO_2) was designed to investigate whether the two helices were brought into close proximity in the presence of different membranes by antiparallel arrangement.

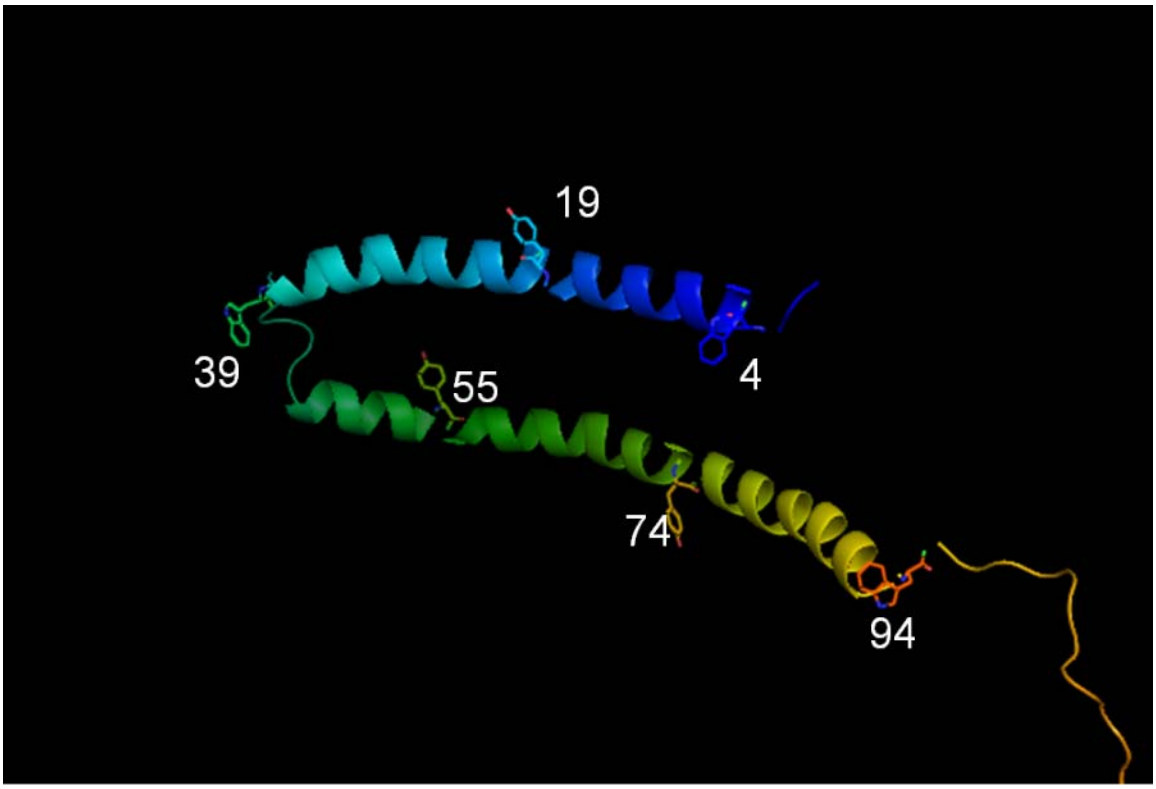

Figure 3.1. The structure of α-syn bound to SDS micelles elucidated by Ulmer et al.[1] Mutations constructed for this study are numbered.

3.3 METHODS

Protein Preparation, Modification, and Characterization.

A single Trp mutation was introduced in three various positions to replace an aromatic amino acid (F4, Y39, and F94) by site-directed mutagenesis. Except for Y39/W94, where three of the four native tyrosines were mutated into phenylalanines, all four tyrosines were mutated to phenylalanines, and an additional tyrosine residue was introduced in four various positions (A19, V55, V74, and F94). All the sequences were confirmed by DNA sequencing (California Institute of Technology DNA Sequencing Core Facility). Expression and purification of mutants were achieved by following protocols outlined in Chapter 1.

Preparation of Membrane Mimics.

SDS micelles and SUVs were fabricated according to procedures located in Chapter 1. SUVs were made from a 1:1 molar mixture of lipids, 1-palmitoyl-2-oleoyl-*sn*-glycero-3-phosphocholine (POPC), and 1-palmitoyl-2-oleoyl-*sn*-glycero-3-phosphate (POPA), following published protocols.[12] The SUVs were characterized by dynamic light scattering.

Dynamic Light Scattering.

The SUVs made from 1:1 POPC:POPA phospholipids were characterized using dynamic light scattering. DLS measurements were made with a 0.1 mg/mL vesicles solution in NaP_i buffer at 25 °C on a PD4043 detector (Precision Detectors,

Inc., Bellingham, MA). The DLS sample was illuminated with a diode laser operating at 658 nm at a scattering angle of 90°. The radii populations were extrapolated from the collected correlation functions by Precision Deconvolve[32] software.

Spectroscopic Measurements.

Prior to preparing samples for measurements, oligomeric materials in the concentrated protein stock were removed by filtration through Microcon YM-100 spin filter units (molecular weight cutoff 100 kD; Millipore). The protein samples were also exchanged into 20 mM NaP_i buffer (pH 7.4). Protein samples (5 μM) were measured at 25 °C. For samples containing SDS micelles and 1:1 POPC:POPA SUVs, a final concentration of 31 mM micelles and 1.4 mg/mL of vesicles were achieved, respectively. Luminscence spectra and time-resolved fluorescence measurements were obtained by methods outlined in Chapter 1. The time-resolved fluorescent energy transfer kinetics were fitted using the NNLS practice.

3.4 RESULTS AND DISCUSSIONS

Dynamic Light Scattering.

Figure 3.2 shows the distance distribution extracted from the DLS correlation functions. The data suggests that the vesicles were uniform in size, with a measured radius of 7.57 nm. Assuming that both SDS micelles and 1:1 POPC:POPA

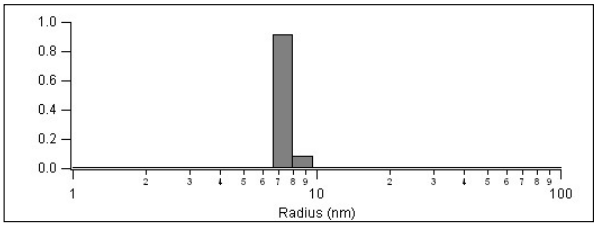

Figure 3.2. The fitted spectra for DLS correlation function of 0.1 mg/mL of 1:1 POPC:POPA SUVs in 20 mM NaP_i buffer (pH 7.4). The average radius for the SUVs is 7.57 nm.

vesicles are perfect spheres, the surface area of the vesicles is more than ten times larger than that of the micelles.

Trp fluorescence.

Trp was incorporated into all the mutants at three different sites (W4, W39, and W94). Trp emission is a useful probe to determine the local environment of Trp.[13-16] **Table 3.1** shows the fluorescence maxima of the Trp mutants and NATA, in NaP_i buffer, SDS micelles, and 1:1 POPC:POPA vesicles. The results shown are similar to the fluorescence maxima reported in previously published work.[17,18] It is shown that the fluorescence maxima in NaP_i buffer are similar between NATA and all Trp mutants.

In the presence of SDS micelles, it is shown all three Trp emissions exhibit a prominent blue shift. This blue shift is indicative that the Trp residues are located in a more hydrophobic environment. Further blue shifts of the fluorescence maxima are only observed when W4 and W94 are introduced into SUVs. On the contrary, there is a slight red-shift in emission for W39 inserted into SUVs vs. micelles. The difference of Trp behavior between micelles and SUVs implies that different structures can be formed when α-syn is associated with the two different membranes.

	λ_{max} (nm)		
	20 mM NaP_i	SDS micelles	1:1 POPC:POPA
NATA	354	352	353
F4W	348	328	326
Y39W	348	338	340
F94W	351	338	335

Table 3.1. Fluorescence maxima of NATA and α-syn mutants in the presence of NaP_i, SDS micelles, and 1:1 POPC:POPA vesicles

Time-resolved fluorescence kinetics.

Since α-syn is unstructured in solution, most of the mutants are expected to have distances longer than 40 Å. **Figure 3.3** to **Figure 3.5** shows the D-A distance populations extrapolated from the time-resolved fluorescence energy-transfer kinetics when the α-syn mutants were in solution (top panel), 1:1 POPC:POPA SUVs (middle panel), and SDS micelles (bottom panel).

W4/Y19(NO_2) and Y19(NO_2)/W39 were mutants used to investigate the behavior of the N-terminal helix when α-syn was present in solution, SUVs, and micelles. **Figure 3.3a** and **3.3b** displays the distances extracted from the experiments. These figures suggest that the size of the N-terminal helix formed when α-syn is associated with 1:1 POPC:POPA and with SDS micelles are comparable. W4/Y19(NO_2) has a population of intermediate polypeptides with distance of 24 Å (~ 50%) in SUVs, compared to 23 Å (~ 50%) in micelles. Similar conclusions can be drawn for Y19(NO_2)/W39 (23 Å, 32% in SUVs vs. 21 Å, 44% in micelles).

The structure of the C-terminal helix was probed by introducing Y39(NO_2)/W94 and Y74(NO_2)/W94. The D-A distances extracted (**Figure 3.4a** and **3.4b**) show distance distributions of these mutants when they were in association with micelles and SUVs. Y39(NO_2)/W94 D-A pair gives ~ 90% of its distance population at > 40 Å (NaP_i and 1:1 POPC:POPA) and ~ 37 Å (SDS micelles). The results imply that the more compact helix is formed when micelles are introduced, rather than SUVs. A similar trend was observed for the Y74(NO_2)/W94 D-A pair. The majority of the polypeptide distance populations when α-syn is associated with SUVs is 28 Å (~ 80%), while with SDS micelles it is 23 Å (~ 60%).

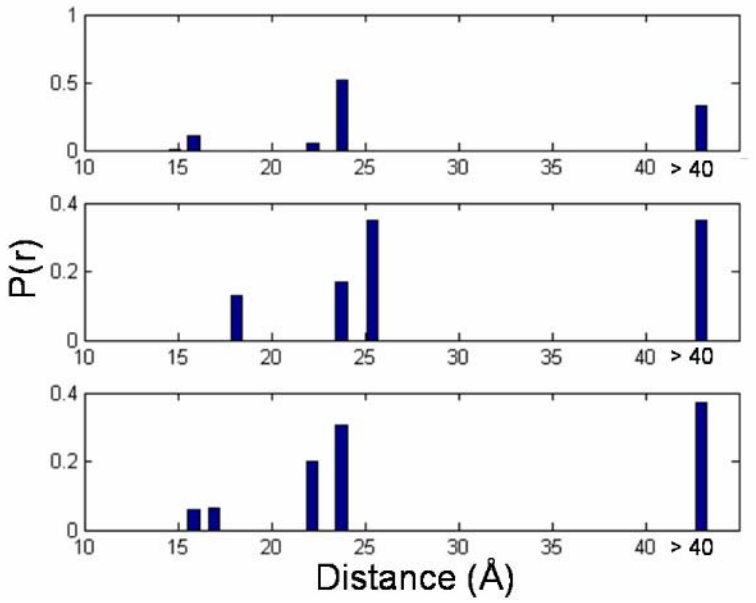

(a)

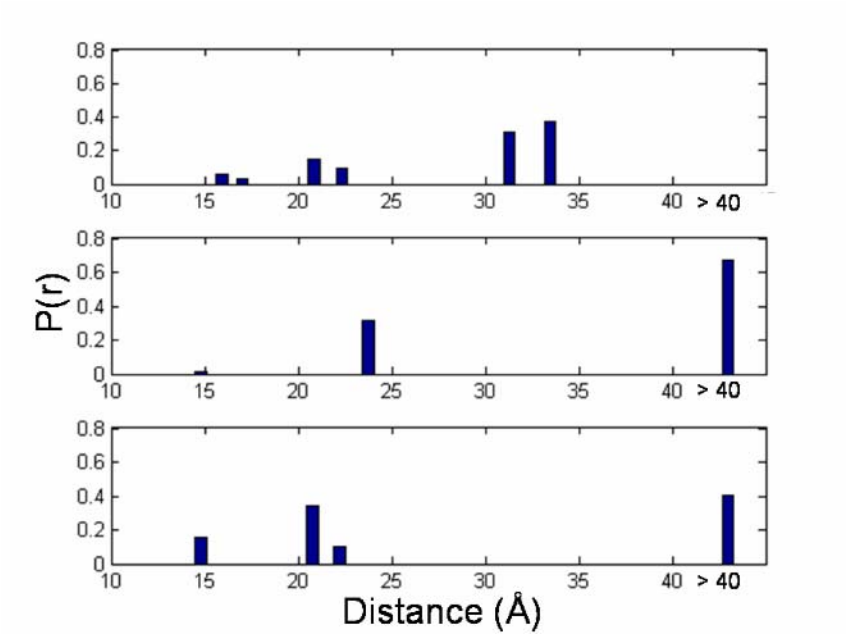

(b)

Figure 3.3. D-A distance distributions extrapolated from FET kinetics for **(a)** W4/Y19(NO_2) and **(b)** Y19(NO_2)/W39 in 20 mM NaP_i buffer (top panel), 1:1 POPC:POPA (middle panel), and 40 mM SDS (bottom panel)

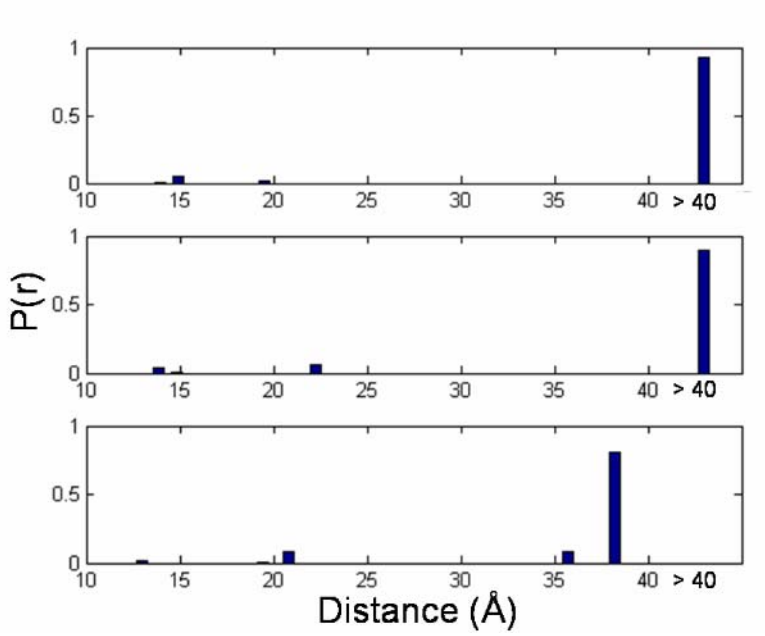

(c)

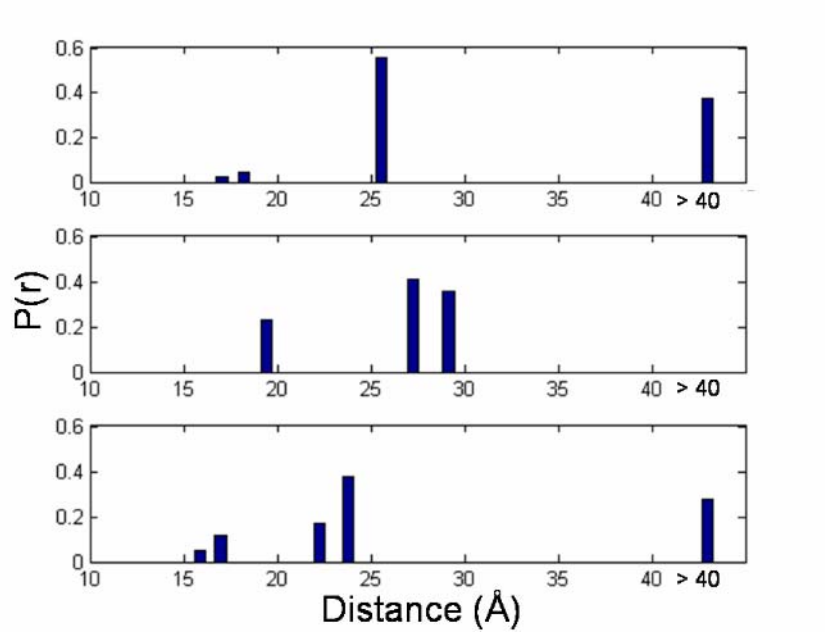

(d)

Figure 3.4. D-A distance distributions extrapolated from FET kinetics for **(c)** Y39(NO_2)/W94 and **(d)** Y74(NO_2)/W94 in 20 mM NaP_i buffer (top panel), 1:1 POPC:POPA (middle panel), and 40 mM SDS (bottom panel)

When comparing the previously published structures of α-syn as associated with SUVs and micelles, the most prominent difference is the arrangement of the two helices. A turn region between residues 38 and 45 brings the two helices in antiparallel arrangement when α-syn is associated with SDS micelles. However, while the linker between the two helices was observed, the helices of α-syn were not brought closer together in the presence of SUVs. Therefore, W4/Y94(NO_2) and W39/Y55(NO_2) were introduced to investigate whether the two helices were brought together in antiparallel fashion.

The W4/Y94(NO_2) mutant is expected to have long D-A distances in NaP_i buffer and SUVs, while the antiparallel motif of the helices should provide a much shorter D-A distance when this α-syn mutant is present in SDS micelles. For W39/Y55(NO_2), W39 is located at the end of the N-terminal helix while Y55(NO_2) is located ten residues from the beginning of the C-terminal helix. Therefore, the D-A distances should be the shortest when the mutant is associated with SDS micelles, followed by SUVs and solution.

Figure 3.5a shows that the extracted distance ensembles confirm this hypothesis. For the W4/Y94(NO_2) mutant, a majority of the distance populations in NaP_i (~ 90%) and SUVs (~ 90%) are longer than 40 Å. However, in the presence of SDS micelles, a significant distance population at ~ 19 Å (~ 30%) and ~ 24 Å (~ 30%) can be observed. In fact, these distances agree with the information provided by Ulmer et al. This implies that the two helices do indeed come into close proximity in the presence of the small SDS micelles. On the other hand, possibly due to the larger size of the SUV, W4 and Y94 are not brought together in such fashion.

For the W39/Y55(NO_2) mutant (**Figure 3.5b**), the ensemble of D-A distances for the micelle-associated structure consists of short (15 Å, 18%), intermediate (21 Å, 44%) and extended (> 40 Å, 38%) polypeptides. The majority of the extracted distances belong to the intermediate polypeptides, agreeing with the proposed distances by NMR micellear structure. On the other hand, the SUV associated structure has a population of short (18 Å, ~ 11%), intermediate (28 Å, ~57%) and extended (> 40 Å, 32%) polypeptides. This above implies that a more compact structure at the turn region is formed when α-syn is associated with micelles than with SUVs, hence matching our prediction. Interestingly, the longest polypeptide observed when the mutant is in NaP_i buffer alone (34 Å, 38%) is much shorter than the ones formed in association with SUVs and micelles. This could be evidence that this turn region has some structural preference in solution and is predisposed to form this turn motif once it is associated with a membrane mimic.

(e)

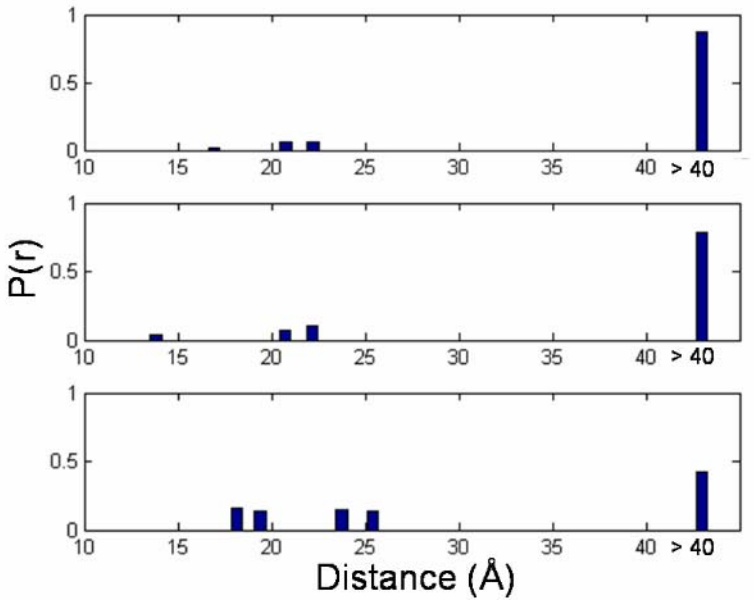

(f)

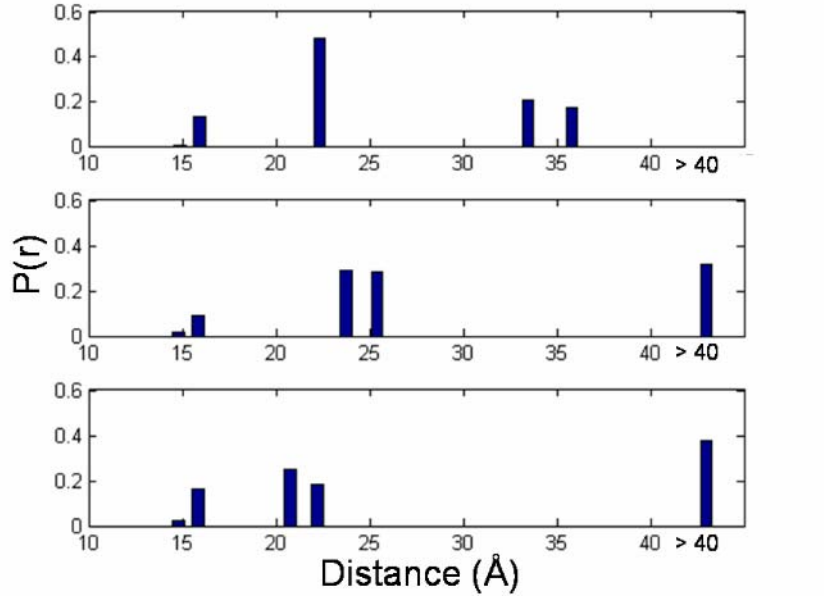

Figure 3.5. D-A distance distributions extrapolated from FET kinetics for **(e)** W4/Y94(NO_2) and **(f)** W39/Y55(NO_2) in 20 mM NaP_i buffer (top panel), 1:1 POPC:POPA (middle panel), and 40 mM SDS (bottom panel)

In conclusion, our results suggest that the linker brings the helices into close proximity when α-syn is in association with SDS micelles. When 1:1 POPC:POPA SUVs were introduced, this phenomenon was not observed. It is also noted that the C-terminal helix is tighter than the N-terminal helix when SDS micelles are present. The opposite phenomenon was observed when SUVs were added. A plausible explanation is that the C-terminal helix has more amino acids (48 residues) to fit into limited spaces than the N-terminal helix (35 residues). Therefore, in small membrane mimics, like SDS micelles, α-syn must create a tighter C-terminal helix for steric purposes. While in association with larger membrane mimics, namely 1:1 POPC:POPA, sterics are no longer an issue and therefore, the C-terminal helix can be relatively relaxed.

3.5 ACKNOWLEDGEMENTS

This work was completed in collaboration with Dr. Jennifer C. Lee.

3.6 REFERENCES

(1) Ulmer, T. S.; Bax, A.; Cole, N. B.; Nussbaum, R. L. *J. Biol. Chem.* **2005**, *280*, 9595–9603.
(2) Jao, C. C.; Der-Sarkissian, A.; Chen, J.; Langen, R. *Proc. Natl. Acad. Sci. U. S. A.* **2004**, *101*, 8331–8336.
(3) Gennis, R. B. *Biomembranes: Molecular Structure and Function*; Springer: New York, 1989.
(4) Bussell, R.; Eliezer, D. *J. Mol. Biol.* **2003**, *329*, 763–778.
(5) Forster, T. *Ann. Phys.-Berlin* **1948**, *2*, 55–75.
(6) Beechem, J. M.; Haas, E. *Biophys. J.* **1989**, *55*, 1225–1236.
(7) Navon, A.; Ittah, V.; Landsman, P.; Scheraga, H. A.; Haas, E. *Biochemistry* **2001**, *40*, 105–118.

(8) Lyubovitsky, J. G.; Gray, H. B.; Winkler, J. R. *J. Am. Chem. Soc.* **2002**, *124*, 14840–14841.
(9) Lee, J. C.; Engman, K. C.; Tezcan, F. A.; Gray, H. B.; Winkler, J. R. *Proc. Natl. Acad. Sci. U. S. A.* **2002**, *99*, 14778–14782.
(10) Wu, P. G.; Brand, L. *Anal. Biochem.* **1994**, *218*, 1–13.
(11) DeLano, W. L. *The PyMOL User's Manual;* Palo Alto, CA. 2002.
(12) Kim, J. E.; Arjara, G.; Richards, J. H.; Gray, H. B.; Winkler, J. R. *J. Phys. Chem. B* **2006**, *110*, 17656–17662.
(13) Reshetnyak, Y. K.; Koshevnik, Y.; Burstein, E. A. *Biophys. J.* **2001**, *81*, 1735–1758.
(14) Kleinschmidt, J. H.; den Blaauwen, T.; Driessen, A. J. M.; Tamm, L. K. *Biochemistry* **1999**, *38*, 5006–5016.
(15) Doring, K.; Konermann, L.; Surrey, T.; Jahnig, F. *Eur. Biophys. J.* **1995**, *23*, 423–432.
(16) Surrey, T.; Jahnig, F. *Proc. Natl. Acad. Sci. U. S. A.* **1992**, *89*, 7457–7461.
(17) Lee, J. C.; Lai, B. T.; Kozak, J. J.; Gray, H. B.; Winkler, J. R. *J. Phys. Chem. B* **2007**, *111*, 2107–2112.
(18) Lee, J. C.; Langen, R.; Hummel, P. A.; Gray, H. B.; Winkler, J. R. *Proc. Natl. Acad. Sci. U. S. A.* **2004**, *101*, 16466–16471.